Available online at www.sciencedirect.com
SCIENCE DIRECT®
PERGAMON
Polyhedron 22 (2003) 2191–2197
POLYHEDRON
www.elsevier.com/locate/poly

# Theoretical studies on the electronic states of electron-doped copper oxides

Taku Onishi *, Daisuke Yamaki, Kizashi Yamaguchi

*Department of Chemistry, Graduate School of Science, Osaka University, Toyonaka, Osaka 560-0043, Japan*

Received 7 October 2002; accepted 11 December 2002

**Abstract**

The infinite layer copper oxides denoted as $ACuO_2$, where A stands for the alkaline earth metal such as strontium or calcium, have attracted much attention in relation to high-temperature ($T_c$) superconductivity. Superconductivities of these species are achieved by several chemical doping such as hole-doping (h-doping) and electron-doping (e-doping). In this study, we have performed hybrid-density functional theory calculations, which are available in the strongly correlated systems such as transition metal complexes, in order to examine the electronic states after one e-doping for the linear chain clusters such as CuOCu and $Cu_3O_2$. The electronic states have been clarified from view points of energy, spin and charge density populations, natural orbital analysis and the difference of density. As the hole-doped electronic states have already been examined for the same clusters by the same methods in our previous work, we discuss the differences of the changes of electronic states between h-doping and e-doping.


*Keywords:* Superconductivity; Electron-doping; HDFT; Infinite layer; Natural orbital; Density

## 1. Introduction

The infinite layer (IL) copper oxides denoted as $ACuO_2$, where A is the alkaline earth metal, were first synthesized by Siegrist et al. [1], and have attracted much attention from the view point of the high-$T_c$ superconductivity. Though the antiferromagnetic $Ca_{0.85}Sr_{0.15}CuO_2$, which is the one kind of $ACuO_2$ discovered by Siegrist et al. has not showed superconductive properties [2], superconductivity by hole-doping (h-doping) [3] and electron-doping (e-doping) [4] were achieved in other IL compounds. In addition, the artificially layered superlattices containing two different IL compounds displayed superconductivity. In $(BaCuO_2)_2/(CaCuO_2)n$ superlattices [5–7], under high oxygen pressure and temperature growth conditions, the $(BaCuO_2)^2$ block, which is much more unstable than the $CaCuO_2$ block, causes the charge reservoir block necessary for superconductivity.

Theoretical treatments of magnetic transition metal oxides attract current interest. In order to calculate the electronic states of such oxides as copper oxides, the electronic correlation effects play crucial roles. Though symmetry adapted approaches such as configuration interaction (CI) [8] are desirable for estimating quantitative constants such as the effective exchange integrals ($J_{ab}$), it is hardly applicable because of much computational time needed, especially for larger clusters. On the other hand, Illas and Martin [9,10] have obtained the $J_{ab}$ values of the binuclear $Ni_2F_{11}$ cluster, which is part of the perovskite transition metal complex such as $K_2NiF_4$ by broken-symmetry pure density functional theory (DFT) methods. They have shown that the calculated $|J_{ab}|$ values are several times larger than experimental results [11]. However, as Becke's half and half (HH) type hybrid-DFT (HDFT) have improved for strong correlation systems, Illas and our group have successfully showed that the $J_{ab}$ values on nickel clusters of $K_2NiF_4$ by HDFT [12,13] are consistent with experimental results. We have also shown the effectiveness of HDFT for the transition metal oxides such as clusters of $La_2CuO_4$ and $K_2NiF_4$ [14].

* Corresponding author. Tel.: +81-6-6850-5405; fax: +81-6-6850-5550.
*E-mail address:* taku@chem.sci.osaka-u.ac.jp (T. Onishi).

0277-5387/03/$ - see front matter 
doi:10.1016/S0277-5387(03)00153-0

The electronic structure of the $CuO_2$ plane is considered to play an important role in achieving the superconductivity of copper oxides. In our previous work [15], we examined the one hole-doped (h-doped) electronic states for the clusters such as CuOCu (**1**), $Cu_3O_2$ (**2**) and $Cu_4O_4$ as the cluster models on $CuO_2$ planes of perovskite-type $La_2CuO_4$ [15]. From its energy diagram, it is concluded that the stability of each spin state after h-doping is explained by both d–p and superexchange (SE) interactions between coppers, and larger clusters should be used when estimating the stability of h-doped electronic states. On the other hand, electron-doped (e-doped) electronic states of copper oxides on the $CuO_2$ plane of IL copper oxides have not been investigated, though the electronic states of $CaCuO_2$ and $SrCuO_2$ before doping were examined by Wu et al. [16]. In this study, we have calculated the one e-doped linear chain models such as **1** and **2** to investigate the electronic states after e-doping. Finally, by comparing both one h-doped and e-doped states, we finally discuss the change of electronic states and the possible mechanism of superconductivity.

## 2. Computational methods

Previously we have applied *ab initio* molecular orbital (MO) methods including electron correlation effects to cluster models of metal complexes such as copper oxides and so on [13–15,17–21]. Especially, we have examined the applicability of HDFT methods based on the Hohenberg–Khon theory [22] and Kohn–Sham equation [23], since they take less computational time compared with other methods such as complete active space configuration interaction and UHF coupled cluster methods. It is found that HDFT methods such as UB2LYP, UB2VWN and US2VWN provide the reliable results of transition metal oxides and halides from the view points of effective exchange integral ($J_{ab}$) values, natural orbitals (NO), spin density distribution and charge density distribution [14]. In this study, we adapt UB2LYP method including the terms of generalized gradient approximations (LSDA and GGA) [24–26] for model clusters of strongly correlated copper oxides. Exchange correlation potentials in HDFT calculations are defined by:

$$E_{XC} = C_1 E_X^{HF} + C_2 E_X^{Slater} + C_3 E_X^{Becke88} + C_4 E_C^{VWN} + C_5 E_C^{LYP} \quad (1)$$

where the second and fourth terms mean exchange and correlation terms, respectively, and the third and fourth terms are the exchange and correlation corrections involving the gradient of the densities by Vosko, Wilk and Nusair (VWN) [27], and Lee, Yang and Parr (LYP) [28], respectively. $C_i$ ($i = 1$–5) are parameter sets ($C_1$, $C_2$, $C_3$, $C_4$ and $C_5$) using (0.5, 0.5, 0.5, 1.0 and 1.0) in UB2LYP methods. We adapt Tatewaki–Huzinaga MIDI [29] plus Hay's diffuse [30] and 6-31G* to copper and oxygen for the basis sets of these calculations, respectively. All calculations have been performed by GAUSSIAN-94 program package [31].

## 3. Structures

For the IL compounds, $(Ca_{0.86}Sr_{0.14})CuO_2$ was first synthesized by Siegrist et al. [32]. They found that this structure was consisted of $CuO_2$ planes separated by Ca and Sr atoms and is a simple defect perovskite with ordered oxygen vacancies. The distance between copper and oxygen on $CuO_2$ planes was decided to be 1.9306 Å by their X-ray diffraction measurement. Later, it was confirmed that there exists an $CuO_2$ plane in another but similar IL compound $(Ca_{0.85}Sr_{0.15})CuO_2$ [33]. Fig. 1 illustrates $CaCuO_2$. In this study, we have constructed model clusters such as CuOCu (**1**) and CuOCuOCu (**2**) on $CuO_2$ plane, which is responsible for sources of magnetic properties, as shown in Fig. 2. These model clusters are the same ones used in the previous HDFT studies on h-doping into $La_2CuO_4$ [15]. Here, we therefore compare the e-doping with h-doping electronic states in the same clusters.

## 4. Results and discussion

### 4.1. Energy, spin density and charge density populations

As shown previously [15], spin densities are populated on $3d_{x^2-y^2}$ orbital of both coppers in the electronic states of **1** before e-doping. The low-spin (LS) state exhibiting the antiferromagnetic interaction is the ground state because of the SE interaction. By e-doping for both its LS and high-spin (HS) states, the electronic states are changed. In the case of the e-doping for the LS state, the two types of states (the e-doped LS I and LS II states) are caused, while the e-doped HS state causes only the spin densities on 4s orbitals on coppers. The e-doped LS I state has the spin densities on 2pσ orbital of oxygen,

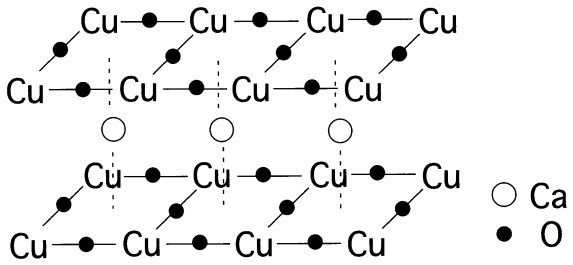


Fig. 1. The layer structures of $CaCuO_2$. The $CuO_2$ plane is common in other copper oxides exhibiting superconductivity.

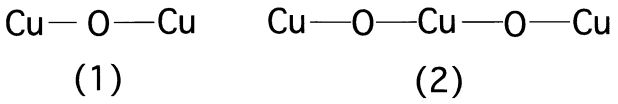


Fig. 2. Cluster models (**1**) and (**2**) of $CuO_2$ plane.

though the spin densities on coppers vanish. On the other hand, the e-doped LS II state has the spin densities on 2pπ orbitals of oxygen and the spin densities on coppers vanish.

Table 1 shows the energy and spin angular momentum of **1** and **2** before and after e-doping. The e-doped LS I and LS II states of **1** and **2** are more stable than the e-doped HS states of **1** and **2**, respectively. Compared with both e-doped LS states, it is found that the 2pπ orbitals of **1** and **2**, which are caused by e-doping, stabilize the clusters more than the 2pσ orbitals of **1** and **2**, respectively. As a result, the e-doped LS II states are more stable than the e-doped LS I states in both **1** and **2**. Table 2 shows the spin and charge densities of **1** and **2** after e-doping. Site numbers are specified as Cu1–O2–Cu3 and Cu1–O2–Cu3–O4–Cu5 for **1** and **2**, respectively. For both **1** and **2**, the larger spin densities are seen on coppers located on the edge of the cluster. It is considered that one doped electron causes the spin densities on 4s orbitals. On the other hand, in the case of both e-doped LS states, the spin densities on oxygen are seen for both **1** and **2**. In addition, coppers located in the edge of cluster have little spin densities. However, in the e-doped LS states of **2**, coppers located in the middle have the spin densities, which is close to 1.0, because one electron is only doped in this case.

### 4.2. Natural orbital analysis

The MO picture is the very useful instrument to analyze the magnetic interactions of the strongly correlated compounds. In order to examine the change of the electronic states after h-doping and e-doping precisely, NO analyses have been performed. NOs are determined by diagonalizing the their first-order density matrices as:

$$\rho(r,r') = \sum n_i \phi_i(r) \phi_i(r')^* \quad (2)$$

where $n_i$ and $\phi_i$ denote the occupation number and NO, respectively. The $n_i$ of bonding and antibonding NOs, $\phi_i$, are close to 2.0 and 0.0, respectively, except for the magnetic orbitals, which are close to 1.0.

Table 1
Energy and spin angular momentum of **1** and **2** after electron-doping by UB2LYP

| Model | Spin state | Energy | Spin angular momentum |
|---|---|---|---|
| CuOCu (**1**) | HS | −3354.8201 | 3.803 |
| | LS I | −3354.9158 | 0.780 |
| | LS II | −3354.9726 | 0.757 |
| $Cu_3O_2$ (**2**) | HS | −5069.9970 | 6.023 |
| | LS I | −5070.0792 | 1.092 |
| | LS II | −5070.1299 | 1.077 |

Figs. 3 and 4 show the shapes and occupation numbers of singly occupied NO (SONO) for e-doped **1** and **2**, respectively. From Fig. 3, 2pσ and 2pπ orbitals play important roles in the e-doped LS I and LS II states, respectively. On the other hand, in the e-doped HS states, 4s orbitals are predominant in SONO−1, though contributions of $3d_{x^2-y^2}$ orbitals are not negligible as shown in both SONO+1 and SONO+0. In the e-doped LS I and LS II states of **2**, 2pσ and 2pπ orbitals are predominant in SONO−1 and SONO+1, respectively, as shown in Fig. 4 and 4s orbitals are seen in SONO−2 and SONO+2 of the e-doped HS state. However, the contribution of $3d_{x^2-y^2}$ orbital of copper in the middle does vanish in both e-doped LS states, interacting with p orbitals of oxygen. All occupation numbers of SONOs become 1.000, showing that no SONOs interact with other SONOs.

### 4.3. The difference of density

Previous studies [15] on h-doping have revealed that the difference of density between before or after h-doping is significant, since the shapes of holes can be expressed pictorially. Similarly, it would be expected that the difference of density between before and after e-doping is a useful index, as the changes of density would be clearly grasped. The difference of density $\Delta\rho$ is defined by

$$\Delta\rho = \rho_{\text{before}} - \rho_{\text{after}} \quad (3)$$

where $\rho_{\text{before}}$ and $\rho_{\text{after}}$ denote the density of before and after e-doping, respectively.

Figs. 5(a) and (b) show the difference of density between before and after e-doping for **1** and **2**, respectively. In Fig. 5(a), the e-doped HS state of **1** has almost no white part, where the density is decreasing, and both coppers have a black part, where the density is increasing. It is found that electron is added only to 4s orbitals in the e-doped HS state of **1**. On the other hand, both e-doped LS states of **1** have a black part in the middle oxygen. It implies that the middle oxygen has 2pσ and 2pπ orbitals in e-doped LS I and LS II states of **1**, respectively. In addition, electron is partially added to $3d_{x^2-y^2}$ orbitals of both coppers. From Fig. 5(b), it is found that electron is added to 4s orbitals of both edge coppers and 2pσ orbitals of oxygen in the e-doped HS state of **2**.

From the view point of spin density populations, it is concluded that the spins on 2pσ orbitals of oxygen are, in the e-doped HS states, little influence and this increase of density has no big effect on magnetic property. On the other hand, both e-doped LS states of **2** cause the increase of 2pσ and 2pπ orbitals of

Table 2
Spin and charge densities[a] of **1** and **2** after electron-doping by UB2LYP

| Model | Spin state | Cu1 | O2 | Cu3 | O4 | Cu5 |
|---|---|---|---|---|---|---|
| CuOCu (**1**) | HS | 1.558 | −0.115 | 1.558 | | |
| | | (0.873) | (−0.748) | (0.873) | | |
| | LS I | 0.131 | 0.738 | 0.131 | | |
| | | (0.814) | (−0.628) | (0.814) | | |
| | LS II | −0.004 | 1.008 | −0.004 | | |
| | | (0.763) | (−0.527) | (0.763) | | |
| $Cu_3O_2$ (**2**) | HS | 1.382 | 0.068 | 1.099 | 0.068 | 1.382 |
| | | (0.828) | (−0.799) | (0.941) | (−0.799) | (0.828) |
| | LS I | 0.089 | 0.509 | −1.195 | 0.509 | 0.089 |
| | | (0.757) | (−0.704) | (0.893) | (−0.704) | (0.757) |
| | LS II | −0.024 | 0.581 | −1.114 | 0.581 | −0.024 |
| | | (0.705) | (−0.688) | (0.967) | (−0.688) | (0.705) |

[a] Charge density in parenthesis.

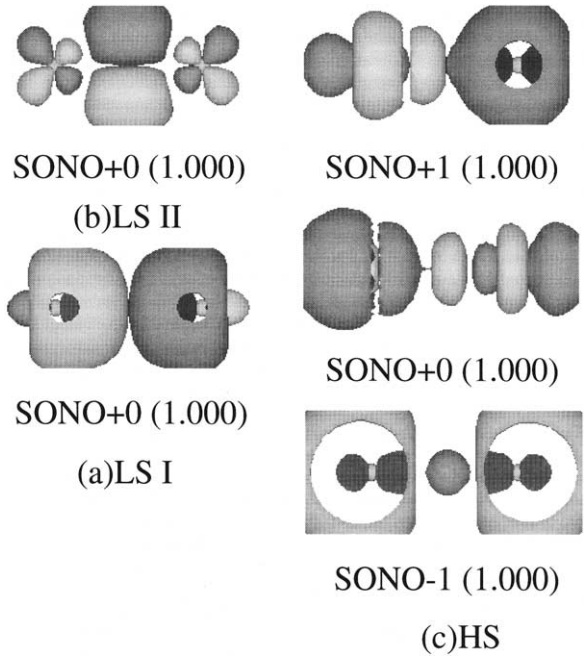


Fig. 3. The NOs and occupation numbers (in parenthesis) of e-doped CuOCu cluster (**1**) in the LS and HS states.

oxygen, and its orbitals play the role of magnetic properties from the existence of spin density on oxygen, as shown in Table 2. However, changes of the density are not seen in the middle copper. This is because one electron is added to the small clusters and the charge transfer from two oxygen to edge coppers has already occurred.

## 5. Concluding remarks

### 5.1. General conclusions

In this study, the changes of electronic state before and after one e-doping are investigated for the linear chain model clusters such as **1** and **2**. In the case of e-doped HS state, electron is added to the 4s orbitals of coppers on both edges, obeying the Hund's rule. On the other hand, in the case of e-doped LS states, electron is added to the $3d_{x^2-y^2}$ orbitals of coppers on both edges, and hole is formed in 2pσ and 2pπ orbitals of oxygen because of charge transfer from oxygen to copper. It is also found that the e-doped LS states are more stable than the e-doped HS state. Compared with both e-doped LS states, it is found that 2pσ spins of oxygen stabilize the clusters more than 2pπ spins.

In the same way as the existence of spins of oxygen stabilizes the clusters in the h-doping, the e-doped LS states are stabilized by the spins of oxygen, because all e-doped HS states are more unstable than all e-doped LS states. Compared with both e-doped LS states, the e-doped LS II is more stable than the e-doped LS I. Considering the interactions between two 2pσ and two 2pπ orbitals on oxygen in e-doped **2**, two 2pσ and 2pπ orbitals on oxygen interacting, and the bonding 2pσ and antibonding 2pσ* orbitals, and the bonding 2pπ and antibonding 2pπ* orbitals form, respectively. The energy gap between 2pσ and 2pσ* is considered to be larger than that between 2pπ and 2pπ*, as shown in Fig. 6. If larger clusters are used, the energy gap in 2pσ orbitals is thought to become larger than in 2pπ orbitals. Though the 2pπ orbitals are more stable than the 2pσ orbitals in the small clusters, it is considered that the larger energy gap will cause parts of 2pσ orbitals to be more stable as shown in Fig. 7.

Though spins on oxygen play an important role in the h-doping, this fact is considered to be true of the e-doped LS states also. As the e-doped HS states are more unstable than all e-doped LS states, it could be concluded that this is also true for all cases in e-doping. In the near future, the stability of two types of 2p orbitals such as 2pσ and 2pπ orbitals, in the h-doping, should be discussed from the various points of view.

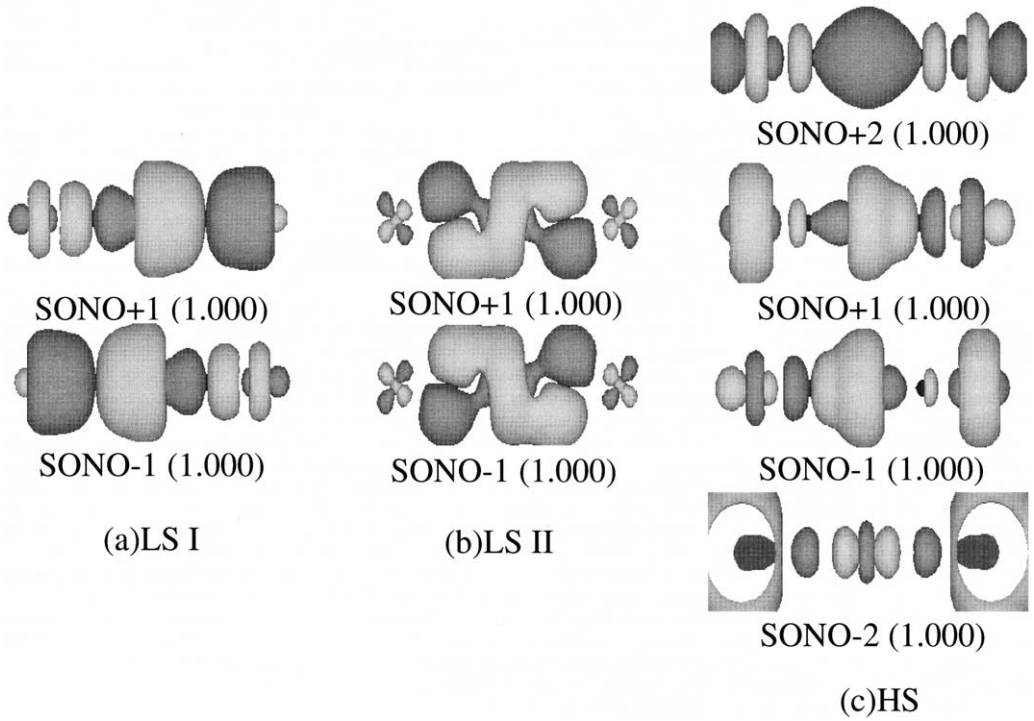


Fig. 4. The NOs and occupation numbers (in parenthesis) of e-doped CuOCu cluster (**2**) in the LS and HS states.

### 5.2. Implications of computational results

The previous and present *ab initio* results on small clusters have revealed that the 2pσ orbital on oxygen plays crucial roles with the coupling of copper 3d orbitals in both h-doped and e-doped copper oxides in the $CuO_2$ plane. In our previous UHF [34,35] and UMP [36] calculations of copper oxides, we have assumed a σ-hole after h-doping in order to construct our J-model for high-$T_c$ superconductivity, leading to singlet superconductivity (SSC) because of the greater stability of the LS state compared to the HS state. The SSC is indeed

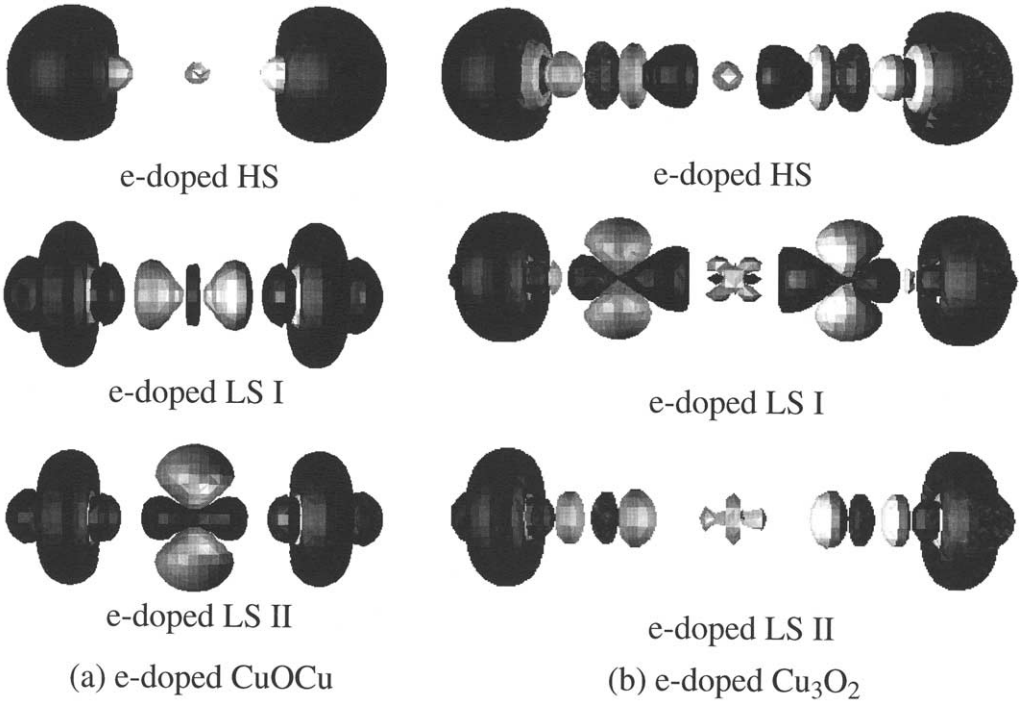


Fig. 5. The difference of density after e-doping of CuOCu (**1**) and CuOCuOCu (**2**) clusters.

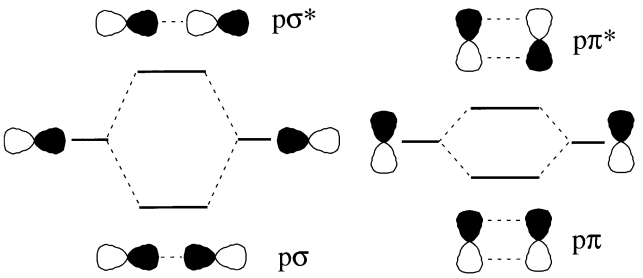


Fig. 6. The orbital interaction schemes of pσ and pπ type orbitals in the $CuO_2$ chain, which determine the energy levels of them (see Fig. 7).

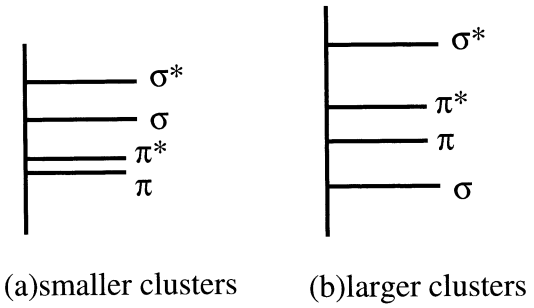


Fig. 7. The orbital energy levels of pσ and pπ type orbitals in smaller and larger clusters of copper oxides.

realized in the case of h-doped copper oxides. The present model calculations also indicates SSC for e-doped copper oxides. Thus our J-model [34,35,37] works well for SSC of both h-doped and e-doped copper oxides.

On the other hand, if the π-hole is assumed after h-doping, the HS state becomes the ground state, suggesting triplet superconductivity [38,39]. It is noteworthy that the π-hole state is more stable than the σ-hole state in the case of GVB calculations of small copper oxide clusters [38,39]. The CASSCF and CI studies of both σ- and π-hole states [40] have indicated that accurate correlation corrections are necessary to elucidate the electronic states and their relative stability. The previous and present results may indicate that the HDFT method such as UB2LYP is applicable to copper oxides with and without h-doping and e-doping. The HDFT studies on larger cluster models of the species are in progress.

## Acknowledgements

This work has been supported by Grants-in-Aid for Scientific Research on Priority Areas (No. 14204061) from the Ministry of Education, Culture, Sports, Science and Technology, Japan. T.O. is also supported by Research Fellowships of the Japan Society for the Promotion of Science for Young Scientists.

## References

[1] T. Siegrist, S.M. Zahurak, D.W. Murphy, R.S. Roth, Nature 334 (1988) 231.
[2] A. Lombardi, M. Mali, J. Roos, D. Brinkmann, Phys. Rev. B 54 (1996) 93.
[3] X.M. Xie, C. Hatterer, V. Mairet, C.F. Beuran, C. Coussot, C.D. Cavellin, B. Eustache, P. Laffez, X.Z. Xu, M. Laguës, Appl. Phys. Lett. 67 (1995) 1671.
[4] M.G. Smith, A. Manthiram, J. Zhou, J.B. Goodenough, J.T. Market, Nature 351 (1991) 549.
[5] S. Colonna, F. Arciprete, A. Balzarotti, G. Balestrino, P.G. Medaglia, G. Petrocelli, Physica C 334 (2000) 64.
[6] G. Balestrino, G. Pasquini, A. Tebano, Phys. Rev. B 62 (2000) 1421.
[7] G. Balestrino, S. Lavenga, P.G. Medaglia, S. Martellucci, A. Paoletti, G. Pasquini, G. Petrocelli, A. Tebano, A.A. Varlamov, Phys. Rev. B 62 (2000) 9835.
[8] F. Illas, J. Casanova, M.A. Garcia-Bach, R. Caballol, O. Castell, Phys. Rev. Lett. 71 (1993) 3549.
[9] R.L. Martin, F. Illas, Phys. Rev. Lett. 79 (1997) 1539.
[10] F. Illas, R.L. Martin, J. Chem. Phys. 108 (1998) 2519.
[11] L.J. de Jongh, A.R. Miedema, Adv. Phys. 23 (1974) 1.
[12] I.P.R. Moreira, F. Illas, Phys. Rev. B 60 (1999) 5179.
[13] T. Onishi, T. Soda, Y. Kitagawa, Y. Takano, D. Yamaki, S. Takamizawa, Y. Yoshioka, K. Yamaguchi, Mol. Cryst. Liq. Cryst. 343 (2000) 133.
[14] T. Onishi, Y. Takano, Y. Kitagawa, T. Kawakami, Y. Yoshioka, K. Yamaguchi, Polyhedron 20 (2000) 1177.
[15] T. Onishi, Y. Takano, D. Yamaki, K. Yamaguchi, Mol. Cryst. Liq. Cryst. 379 (2002) 507.
[16] H. Wu, Q. Zheng, X. Gong, H.Q. Lin, J. Phys: Condens. Matter 11 (1999) 4637.
[17] M. Mitani, Y. Takano, Y. Yoshioka, K. Yamaguchi, J. Chem. Phys. 111 (1999) 1309.
[18] M. Mitani, D. Yamaki, Y. Yoshioka, K. Yamaguchi, J. Chem. Phys. 111 (1999) 2283.
[19] M. Mitani, H. Mori, Y. Takano, D. Yamaki, Y. Yoshioka, K. Yamaguchi, J. Chem. Phys. 113 (2000) 4035.
[20] M. Mitani, D. Yamaki, Y. Takano, Y. Yoshioka, K. Yamaguchi, J. Chem. Phys. 113 (2000) 10486.
[21] T. Soda, Y. Kitagawa, T. Onishi, Y. Takano, Y. Shigeta, H. Nagao, Y. Yoshioka, K. Yamaguchi, Chem. Phys. Lett. 319 (2000) 223.
[22] P. Hohenberg, W. Kohn, Phys. Rev. 136 (1964) B864.
[23] W. Kohn, L.J. Sham, Phys. Rev. 140 (1965) A1133.
[24] J.M. Seminario, Politzer (Eds.), Theoretical and Computational Chemistry, Modern Density Functional Theory: A Tool for Chemistry, vol. 2, Elsevier, Amsterdam, 1995.
[25] J.M. Seminario (Ed.), Theoretical and Computational Chemistry, Recent Developments and Applications of Modern Density Functional Theory, vol. 4, Elsevier, Amsterdam, 1996.
[26] J.M. Seminario (Ed.), Density Functional Theory, Adv. Quantum. Chem, vol. 33, Academic Press, San Diego, CA,, 1998.
[27] S.H. Vosko, L. Wilk, M. Nusair, Can. J. Phys. 58 (1980) 1200.
[28] C. Lee, W. Yang, R.G. Parr, Phys. Rev. B 37 (1988) 785.
[29] H. Tatewaki, S. Huzinaga, J. Chem. Phys. 72 (1980) 4339.
[30] P.J. Hay, J. Chem. Phys. 66 (1977) 4377.
[31] Gaussian 94, M.J. Frisch, G.W. Trucks, H.B. Schlegel, P.M.W. Gill, B.G. Johnson, M.A. Robb, J.R. Cheeseman, T.A. Keith, G.A. Petersson, J.A. Montgomery, K. Raghavachari, M.A. Al-Laham, V.G. Zakrzewski, J.V. Oritiz, J.B. Foresman, J. Cioslowski, B.B.Stefanov, A. Nanayakkara, M. Challacombe, C.Y. Peng, P.Y. Ayala, W. Chen, M.W. Wong, J.L. Baker, J.P. Stewart, M. Head-Gordon, C. Gonzalez, and J.A. Pople, Gaussian, Inc., Pittsburgh, PA, 1995.

[32] T. Siegrist, S.M. Zahurak, D.W. Murphy, R.S. Roth, Nature 334 (1988) 231.
[33] D. Vaknin, E. Caignol, P.K. Davies, J.E. Fischer, D.C. Johnson, D.P. Goshorn, Phys. Rev. B 39 (1989) 9122.
[34] K. Yamaguchi, Y. Takahara, T. Fueno, K. Nasu, Jpn. J. Appl. Phys. 26 (1987) L1364.
[35] K. Yamaguchi, Y. Takahara, T. Fueno, K. Nasu, Jpn. J. Appl. Phys. 26 (1987) L2037.
[36] K. Yamaguchi, Y. Takahara, T. Fueno, K. Nasu, Physica C153–155 (1988) 1213.
[37] K. Yamaguchi, Int. J. Quant. Chem. 37 (1990) 167.
[38] Y. Guo, J.-M. Langlois, W.A. Goddard, III, Nature 239 (1988) 896.
[39] G. Chen, W.A. Goddard, III, Nature 239 (1988) 899.
[40] S. Yamamoto, K. Yamaguchi, K. Nasu, Phys. Rev. B42 (1990) 266.